JOURNAL OF CATALYSIS 76, 405–417 (1982)

Influence of Metal Dispersion on Selectivity and Kinetics of Phenylacetylene Hydrogenation Catalyzed by Supported Palladium

G. CARTURAN,* G. FACCHIN,* G. COCCO,† S. ENZO,† AND G. NAVAZIO‡

*Centro di Chimica Metallorganica del C.N.R., Istituto di Chimica Industriale, Via Marzolo 9, Padova, Italy, †Istituto di Chimica Fisica, Università di Venezia, Calle Larga 2137, S. Marta, Venezia, Italy, and ‡Istituto di Chimica Industriale, Università di Padova, Via Marzolo 9, Padova, Italy

Received November 19, 1981; revised March 2, 1982

Several Pd metal dispersions on vitreous supports and on charcoal have been prepared and used in the half-hydrogenation of phenylacetylene. The metal particle size distributions have been determined both by small angle X-ray scattering (SAXS) and wide angle X-ray scattering (WAXS). The degree of dispersion was dependent on the nature of the support; in the most favorable cases the Pd load was dispersed in metallic particles smaller than 30 Å in diameter. These catalysts hydrogenate phenylacetylene under mild conditions in heptane suspension. The kinetic results indicate that both half-hydrogenation rate and selectivity were largely affected by the degree of dispersion of Pd: a considerable reduction of catalytic effectiveness and selectivity has been observed as the averaged particle diameter was increased. Results have been interpreted and discussed in terms of hydrogen availability on the reacting catalytic center and of the metallic phase features.

INTRODUCTION

Some fundamental chemical processes require large amounts of olefins of reagent grade purity with a very low content of alkynes. Actually this latter requirement can be fulfilled by several methods; for instance, the removal of small amounts of acetylene from the C_2 fraction of gas mixtures is performed by selective solvents (*1*) or by sorption on Cu(I) and Cu(II) salt solutions (*2*). The half-hydrogenation of the alkynes in fluxing systems with chromium–nickel, Pd on silica or cobalt molybdate catalysts (*3*) is also widely used.

The selective removal of acetylenes by hydrogenation with metallic catalysts is naturally dependent upon the energetics of the surface process; however, in spite of the stronger adsorption of alkynes on the metallic surface, i.e., their favorable adsorptive thermodynamic factor with respect to olefins (*4, 5*), the selectivity in the half-hydrogenation of acetylenes rarely reaches the required low percentage of alkynes without notable formation of saturated hydrocarbons even with the best catalysts (*6, 7*). Besides, the difference between the free energies of adsorption of the above mentioned species does not account for the very high selectivity sometimes attained in industrial experience (*8*).

The partial hydrogenation of alkynes with conventional Pd catalysts, a frequent catalytic partner in industrial chemical processes, is affected by several different factors. The outstanding property of Pd to absorb hydrogen and the possible key role of α and β hydride phases in modifying the state of the metal and therefore its selectivity has been thoroughly inspected and put in the right prospective by Palczewska *et al.* (*9–11*). Moreover, the general pattern of selectivity shown by the group VIII metals in the hydrogenation of polyunsaturated organic substrates has been surveyed by Wells (*12*) in terms of relative amounts of hydrogen occupancy in these metals. It has resulted in further insight into preparative factors, related physical characteristics, and ultimately into dependent hydrogen availability on the reacting active sites. Also related to this point are the dynamic processes of formation of the Pd hydride

0021-9517/82/080405-13$02.00/0

phases (*9*), and the PdH stoichiometry (*10, 13–15*) which, under catalytic conditions, are in turn intimately connected to the metal particle size and its morphology.

These facts suggest that large changes in product distribution could be expected depending on the supported metal dispersion. It is noteworthy that among the best Pd supported catalysts used on industrial scale in the selective hydrogenation of alkynes the metal loading is extremely low (0.01–0.03 wt%) (*3*) and it is reasonable to assume that the metal should be highly dispersed.

In the attempt to establish the effectiveness of Pd catalysts in the semihydrogenation of alkynes, we extended to phenylacetylene our previous study on the selectivity of Pd catalysts dispersed on vitreous supports in the hydrogenation of olefins (*16*). Particular care was taken to the microparticle features and to the metal–substrate interactions which, from above mentioned considerations, should be two independent and eventually synergic parameters in the selective hydrogenation of alkynes.

Correlations between catalytic performance and state of the dispersed metal are made difficult by uncertainties in the physical state specification especially in the presence of highly dispersed palladium. Detailed structural investigation on routinely prepared Pd catalysts has revealed the structurally complex nature of the supported samples and the difficulty in achieving very homogeneous states of dispersion (*17–19*). Actually, various ranges of size were distinguished in the particle size distribution functions: thus, large dimensions were found, together with highly divided metal, preventing definite correlations between fine chemical and structural aspects to be achieved.

In order to overcome these difficulties, several Pd catalysts were prepared. Methods previously reported give the chance to obtain very narrow Pd particle size distributions ranged at low diameter values (*18–20*). Moreover, in determining the metal particle distribution function from small angle X-ray scattering (SAXS), no a priori assumption was imposed on the shape of the size distribution function, avoiding the loss of the detailed information content on the real physical state of the dispersion.

EXPERIMENTAL

All chemicals were analytical grade products; phenylacetylene and styrene were commercially available and have been distilled before use. Solvents were dried and distilled under a nitrogen atmosphere. $Pd(C_3H_5)_2$ was synthesized by the reported procedure (*21*). The vitreous supports were obtained by the general procedure already described in our previous papers (*22, 23*): ethanolic solutions of $Si(OEt)_4$, $Al(OBu^{sec})_3$, and NaOMe in the ratio $SiO_2/Al_2O_3/Na_2O = 71/18/11$ were hydrolyzed to a gel. This, on heating up to 250°C, gave the vitreous supports which were ground in a ball-mill. A 200–250 mesh fraction was used. The catalysts were synthetized as previously described (*23, 24*) by reacting the appropriate amount of $Pd(C_3H_5)_2$ in pentane solution with the surface OH groups of the support and reducing with H_2 at room temperature. After solvent evaporation under reduced pressure (10^{-2} mm Hg) the obtained dry catalysts have been stored under nitrogen. The Pd on charcoal catalysts have been prepared according to the usual procedure by impregnation with H_2PdCl_4 and reduction with CH_2O. The working techniques for air sensitive compounds were used throughout all the work.

Kinetics

The kinetic experiments of hydrogenation were carried out at constant H_2 pressure at 25°C. This temperature was mantained by appropriate jackets connected to the external circulation of a thermostat. The reaction vessel was a glass cylinder connected with a three-necked head which allowed the transfer of the catalyst, solvent, and substrate under H_2 or N_2 pressure, and mechanical stirring.

At high H_2 pressure the vessel containing

the N_2 degassed reaction mixture was placed inside a high-pressure cylinder. The reaction was started by connecting with a large high-pressure H_2 reservoir. The kinetic run was followed by drawing the samples of the reaction mixture through a capillary device. These were analyzed by gas liquid chromatography (GLC) on a HP 5730A gas chromatograph equipped with an automatic integrator. At 1 atm of H_2 pressure the reaction was started adding under H_2 with a syringe the desidered amount of substrate to the catalyst suspension; the progress of the reaction was followed by a standard gas uptake apparatus connected with the reaction vessel. Simultaneously the relative percentages of the components in solution were measured withdrawing an appropriate number of samples from the reaction mixture. A good agreement between the two methods has been obtained in all cases.

Efficient stirring was performed by a Teflon-coated magnetic stirrer and by a powerful mechanical shaker and/or stirrer. By using different rates of stirring, it has been possible to determine the experimental conditions under which diffusion affects the kinetic data. The kinetics were performed with stirring rates so high as to avoid possible diffusion interferences.

Surface Area and Pd Metal Dispersion Measurements

SAXS procedure. The SAXS measurements were carried out as previously described (*18, 19*). A Kratky camera equipped with a 80 μm entrance and a 150 μm in front of the detector window and a special 2 × 12-mm line focus X-ray tube was used. A scintillation counter in connection with a pulse height discriminator set to Mo$K\alpha$ line served as the detecting device. The scattering intensity was automatically recorded providing as a rule that 10^5 counts were accumulated at a given angle to measure the intensity scattered by both the catalyst and the corresponding support. The absolute intensity was measured by means of a Lupolen Standard supplied by Kratky laboratory (*25*). Destructive interference due to holes and metal scattering was minimized by absorption of suitable concentrations of *syn*-$C_2H_2Br_2$ of electron density very similar to that of glass and charcoal (electron density of $C_2H_2Br_2$ = 0.998 g electrons/cm^3; glass = 0.95 g electrons/cm^3; charcoal = 1.00 g electrons/cm^3). The small angle X-ray scattering due to the metal particles was obtained by subtracting the scattering of a similarly treated support in order to eliminate both the contribution of occluded pores and the high angle diffuse intensity associated with the tail of the first broad Bragg halo which results from disorder within the support structure. By plotting $h^3J(h)$ vs h^3 ($J(h)$ is the slit-smeared intensity; h is diffusion parameter defined as $4\pi\sin\vartheta/\lambda$ with λ = X-ray wavelength and 2ϑ = scattering angle), it was found that the Porod relation (*26*) was actually satisfied in a relatively large range of h values by nearly all samples. Figure 1 reports the smoothed $h^3J(h)$ vs h curve for samples A_1 and A_3. The contribution of the first part of the scattering curves was calculated by means of the Guinier approximation (*27*), whereas the Porod law was employed for the outer one.

The particle size volume distribution

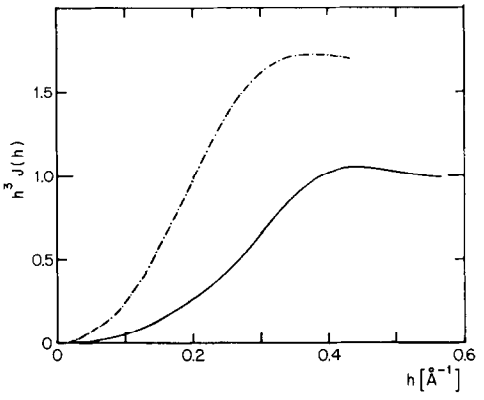

FIG. 1. Plot of $h^3J(h)$ vs h for A_1(———) and A_3 (–·–·–·–) catalysts. These SAXS curves represent the experimental trends after subtracting the scattering of the support material.

function was obtained by the equation:

$$D_V(R) \propto R \int_0^\infty [h^3 J(h) - K] [2J_0(hR) + J_1(hR)(hR - 3/hR)]dh$$

derived from Debye correlation function and standing for the slit-smeared intensity (*28*). $K = \lim_{h\to\infty} h^3 J(h)$ and J_0 and J_1 are the first kind Bessel functions of zero and first order, respectively.

The specific surface expressed in square meters per gram was calculated going into absolute intensity measurements (*24*) according to:

$$S_{sp} = \frac{16\pi^2 \lim_{m\to\infty} m^3 J(m)}{a^2 \lambda^4 r_e^2 N_A P_0 (\Delta p)^2 P}$$

where $J(m)$ is the slit-smeared intensity (n_e^2 cps cm^{-2}, n_e stands for the number of electrons, and cps for counts per second); r_e^2 is the Thomson factor (cm^2); N_A is the Avogadro number; P_0 is the energy per cm of length of the primary beam weakened by the scattering sample and determined by the calibration sample method; p is the sample thickness obtained by multiplying the sample concentration (g cm^{-3}) by the sample holder thickness (cm); a is the distance between the sample and the recording plane (cm).

The volume fraction c of the scattering heterogeneities is available for the slit-smeared intensity according to the relationship:

$$(\Delta p)^2 c(1 - c) = \frac{2\pi \int_0^\infty mJ(m)\, dm}{r_e^2 N_A^2 \lambda^3 a P_0 p}.$$

The Porod diameter, D_p

$$D_p = \frac{3 \int_0^\infty hJ(h)\, dh}{2(1 - c)\lim_{h\to\infty} h^3 J(h)}$$

may be used to represent an average linear dimension of these scattering heterogeneities.

WAXS procedure. The samples were observed in a stainless-steel mounting block (*15*) on a Philips powder diffractometer connected to a highly stabilized generator with a X-ray tube working at 2 kW. Ni filtered Cu$K\alpha$ radiation, Soller slits, a graphite focusing crystal as a monochromator and a scintillation counter supplied with a pulse analyzer were employed. For catalysts of type B and C the reflections were strong enough to allow a Fourier analysis according to recently reviewed procedures (*19, 29*). Intensities of different Pd reflections were scanned in the suitable ranges with a step of 0.02 or 0.05° in 2θ providing that 40,000 counts per point were accumulated. Care was taken to recover the tails of the studied profiles from the background due to the scattering of support material, which was independently recorded under the same experimental conditions. The intensity profiles of the Bragg reflections obtained after subtraction of the support were deconvoluted from the instrumental and spectral effects according to the method of Stokes (*30*) in the Fourier domain. The resultant coefficients $A(L)$, where $L = nd_{hkl}$ is the distance normal to the reflecting (hkl) plane, are the product of a particle size coefficient $A^P(L)$ and a microstain coefficient $A^\epsilon(L)$. The particle size distribution may be extracted from $A(L)$ by the analysis of two reflections when a multiple order series is experimentally available, since $A^\epsilon(L)$ depends on interplanar spacing while $A^P(L)$ does not (*31*). Alternatively a single profile analysis technique may be used (*19, 32*). From the initial slope of $A^P(L)$ vs L curve the average particle size (surface weighted) is determined. These data may be further analyzed to obtain the volume crystallite size distribution (*33*) $p_V(D)$ according to:

$$p_V(D) = \left[D \frac{d^2 A^P(L)}{dL^2} \right]_{L=D}.$$

RESULTS AND DISCUSSION

The hydrogenation of phenylacetylene was studied examining the kinetic behavior of the reaction at constant H_2 pressure as a function of the Pd metal concentration on the support, the weight of catalyst, the Pd

metal particle size distribution on the support, and at different constant H_2 pressures.

Catalyst Features

The Pd metal was supported on the vitreous materials prepared from Na, Si, and Al alkoxides and on charcoal. The ability to prepare $Na_2O/SiO_2/Al_2O_3$ amorphous supports holding a large number of –OH groups on the surface is a fundamental requirement in order to produce high Pd metal dispersions. This fact results from already reported observations (*16, 18*). $Pd(C_3H_5)_2$ reacts with the surface –OH of the support to give a monomolecular dispersion of organometallic species; the $Pd(C_3H_5)_2$ eventually exceeding the surface –OH content is sorbed on the surface of the supports, which hold a large specific surface area; both sorbed $Pd(C_3H_5)_2$ and anchored species can be easily reduced by H_2. In agreement with Yermakov's results the diameters of the Pd metal particles obtained by reducing simply sorbed $Pd(C_3H_5)_2$ are larger than in the case where the organometallic precursor chemically interacted with the surface –OH groups (*16*). Thus, the average metal particle diameter is directly related to the surface –OH group content which is largely affected by the experimental conditions used during the hydrolysis of the solution of the alkoxides. By changing these conditions, we prepared two vitreous supports, namely A and B, having different physical and chemical surface properties. In the preparation of the support A, the alkoxide mixture (50 g of $SiO_2/Al_2O_3/Na_2O$ in the ratio 71/18/11) kept under reflux was reacted with 30 ml of H_2O and 7 ml of 2,4-pentanedione. This latter prevents the immediate separation of the gel obtained by further heating under reflux. In the preparation of the support B a smaller amount of H_2O was used (10 ml).

The characterization of the supports and catalysts was perfected on the basis of properties and data reported in Table 1.

The surface area of the supports was determined by SAXS; the surface –OH groups were determined by reacting the supports with LiH in tetrahydrofuran suspension. The larger concentration of the –OH groups in the support A may be related to the stronger hydrolysis conditions used

TABLE 1

Physical and Chemical Properties of Supports and Catalysts

Sample	–OH[a] (ml H_2 g^{-1})	Surface area[b] (m^2 g^{-1})	Pd%[c]	D_P[d] (Å)	Physical state of the metal	
					Before catalysis	After catalysis
A (support)	16.2	330	—	—	—	—
A_1	—	—	0.67	13	α	α
A_2	—	—	1.61	16	α	α
A_3	—	—	2.27	19	α	$\alpha + \beta$ traces(?)
B (support)	4.9	520	—	—	—	—
B_1	—	—	0.85	21	α	$\alpha + \beta$
B_2	—	—	1.42	27	α	$\alpha + \beta$
C (charcoal)	—	860	—	—	—	—
C_1	—	—	1.72	54	α	β(4.046[e])
C_2	—	—	5.0	106	α	β(4.050[e])

[a] Determined by the reaction support/–OH + LiH → support/–OLi + H_2; data report the amount of H_2 evolved in 1 hr.

[b] Determined by SAXS.

[c] From elemental analysis.

[d] Porod's diameter.

[e] Lattice parameter, Å; see Ref. (*15*).

during the transition from the solution of the parent alkoxides to the gel. Consistently, the Pd metal dispersions obtained on this support are very high and the Porod's diameter, D_P, ranges from 13 to 19 Å. The Pd metal particle size distribution of samples A_1 and A_3 have been investigated in details by SAXS. In the first case (Fig. 2) the distribution is strictly monomodal and in fact it is one of the best dispersions we have been able to prepare. Sample A_3, holding 2.27% Pd, shows two maxima centered at ~15 and ~40 Å in the area ratio 85/15 (Fig. 3). This may be related to the high Pd loading since the reacting $Pd(C_3H_5)_2$ may exceed the surface –OH group content; the small fraction simply sorbed on the surface, upon reduction with H_2, results in the metal particles with diameter ranging from 25 to 55 Å. This interpretation is in agreement with previous results (*16*) and it is confirmed by the Pd dispersions obtained on support B holding a lower –OH group content. In this case the Porod's diameter of the Pd metal particles is larger than the one of samples of A type. The particle size distribution of sample B_2 is shown in Fig. 4 (full line); the ratio between the amount of metal with particle size in the range <30 Å and in the range 30–80 Å is ~50/50. Pd on

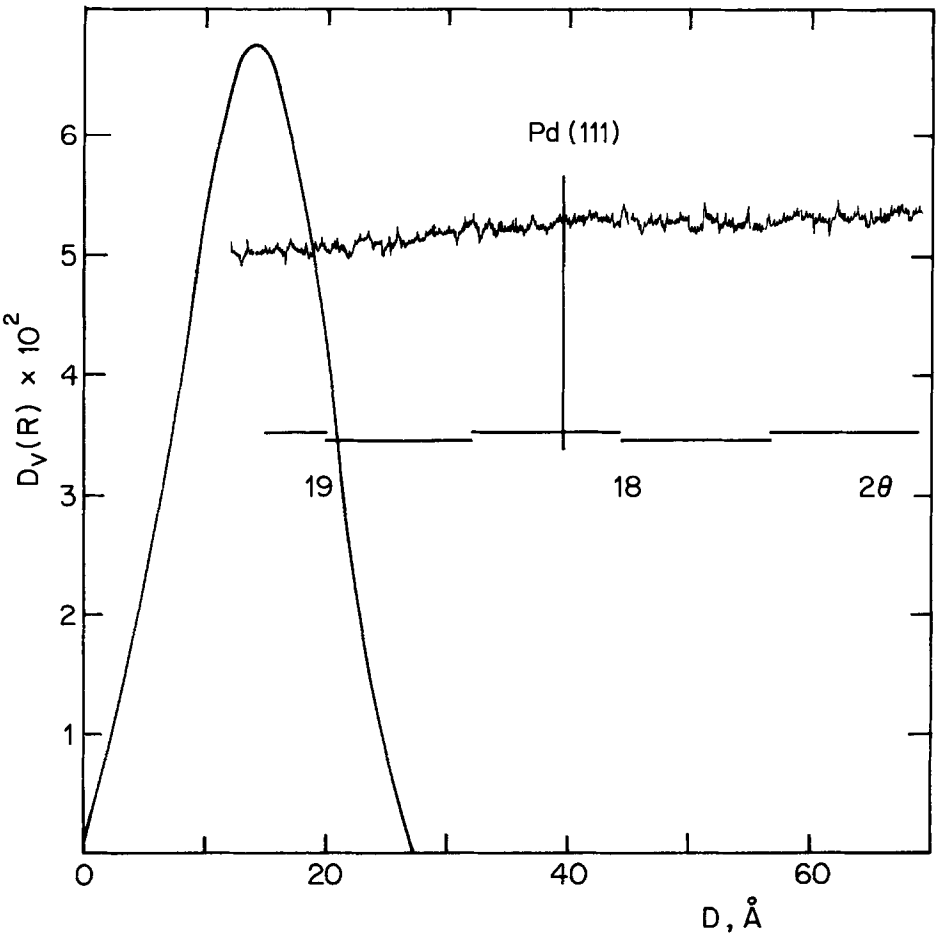

FIG. 2. SAXS particle size distribution for sample A_1. The inside reported diagram refers to the X-ray diffraction profile of the 111 Pd peak for the same catalyst after catalysis. 111 line position of Pd is also quoted as a reference. Mo$K\alpha$ radiation has been employed in this case.

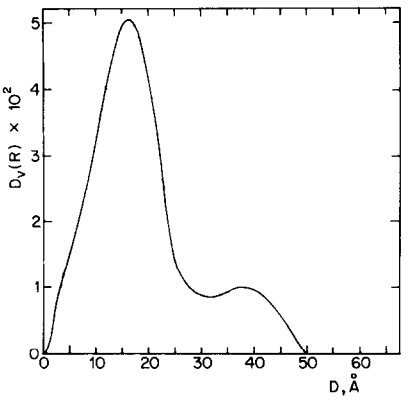

FIG. 3. SAXS volume particle size distribution function for catalyst A_3.

charcoal catalysts display much larger Porod's diameters. The Pd particle size distribution of sample C_2, holding 5.0% Pd (Fig. 5, full line), indicates that the metal is dispersed within a large interval up to 200 Å.

For samples B_2 and C_2 in Figs. 4 and 5 the crystallite size distribution obtained by WAXS (dotted line) are also reported. The good agreement with SAXS data indicates that the Pd metal particles are constituted by single crystallites.

The physical state of the metal on the prepared catalysts has been determined by the corresponding X-ray diffraction patterns. In all cases (Table 1) for catalysts as prepared and stored under N_2, the unique phase present was α PdH and therefore the atomic percentage of dissolved hydrogen should not exceed 1% (*34*). After the catalytic run at 1 atm of H_2 pressure the decanted catalyst have been transferred under H_2 into the stainless-steel sample holder and examined; while catalysts A_1, A_2, and A_3 still display α PdH as the unique discernible phase (Fig. 2 inside reported pattern), a sure evolution to β PdH occurred in the C_1 and C_2 cases for which the lattice constants have been reported in Table 1. The B_1 pattern is shown in Fig. 6; it results that the 111 line position does not allow a definite attribution of the physical state of the metal, however, the observed shift of the peak manifests the high hydrogen content modifying the original Pd lattice. In Table 1, $\alpha + \beta$ stands as a symbol to individualize this structural feature. For catalyst A_3 also reported in Fig. 6 the line shift is less marked suggesting a structural situation near to α PdH.

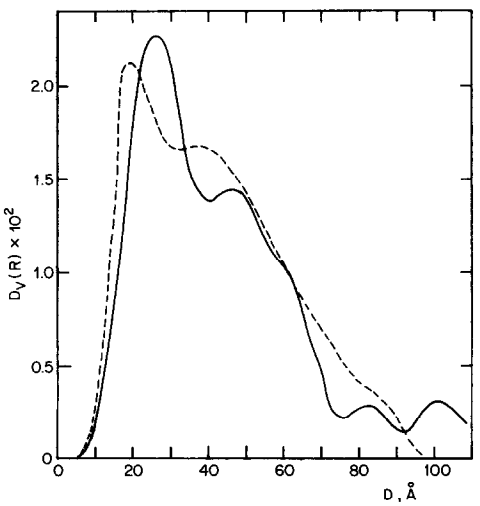

FIG. 4. WAXS volume crystallite (----) and SAXS volume particle (———) size distribution functions for the B_2 sample.

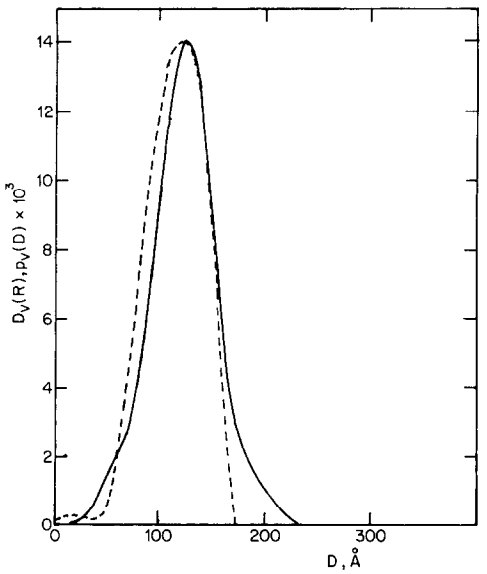

FIG. 5. WAXS volume crystallite (– – – –) and SAXS volume particle (——) size distribution functions for the C_2 sample.

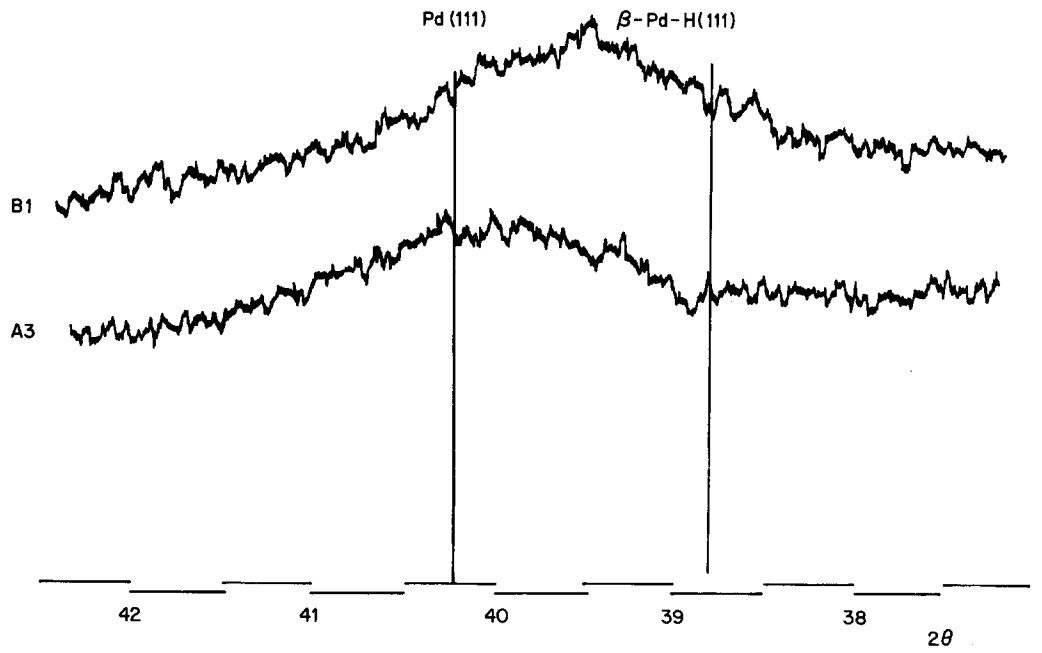

FIG. 6. X-Ray diffrection profile (Cu$K\alpha$ radiation) of the 111 Pd peak for catalysts A_3 and B_1 after catalytic hydrogenation. The 111 line positions of Pd and β PdH are quoted as a reference.

Kinetic Behaviour and Selectivity

In all kinetic experiments the PhC_2H hydrogenation leads ultimately to the formation of ethylbenzene (Fig. 7A). Independent measurements of the hydrogenation of styrene at 1 atm of H_2 pressure with the catalysts of type A and B (Fig. 7B) indicated that the rate law was unaffected by the olefin concentration since a linear trend of the plot of percentage styrene vs time was observed. This result was expected: in fact it is the typical behavior of the hydrogenation of olefins with Pd catalysts under constant H_2 pressure (*23, 35, 36*), the reaction being independent on the concentration of the substrate. Since a linear trend was also found for the phenylacetylene half-hydrogenation, within a large range of percentage of conversion to styrene (Fig. 7A), both PhC_2H and PhC_2H_3 hydrogenation rates can be expressed as the zeroth order rate constants $k_{obs\ PhC_2H}$ and $k_{obs\ PhC_2H_3}$, respectively. These constants were also obtained from volumetric measurements based on H_2 consumption: the calculation of k_{obs} for PhC_2H and PhC_2H_3 within the same kinetic run has been possible since the catalysts of type A and B were selective enough to keep the two hydrogenation reactions quite separated. A typical comparison among the rate constants from GLC and from volumetric H_2 consumption is shown in Fig. 7 for catalyst B_2; it indicates a good agreement between the different experiments. The reproducibility of the experiments—the variation being not larger than 3% from one $C_6H_5 \cdot C_2H$ charge to another using the same catalyst charge and 2% for replicate kinetic experiments—and the relatively low standard deviations on k_{obs}—never exceeding 7%—gives full confidence to the data reported in Table 2.

The kinetics of the hydrogenation of PhC_2H with catalysts C_1, C_2 and with catalysts B_2 at high H_2 pressure do not allow the determination of $k_{obs\ PhC_2H_3}$ (Figs. 8 and 9). Styrene is largely present during the hydrogenation process, although the obtained data indicate that the values of $k_{obs\ PhC_2H_3}$

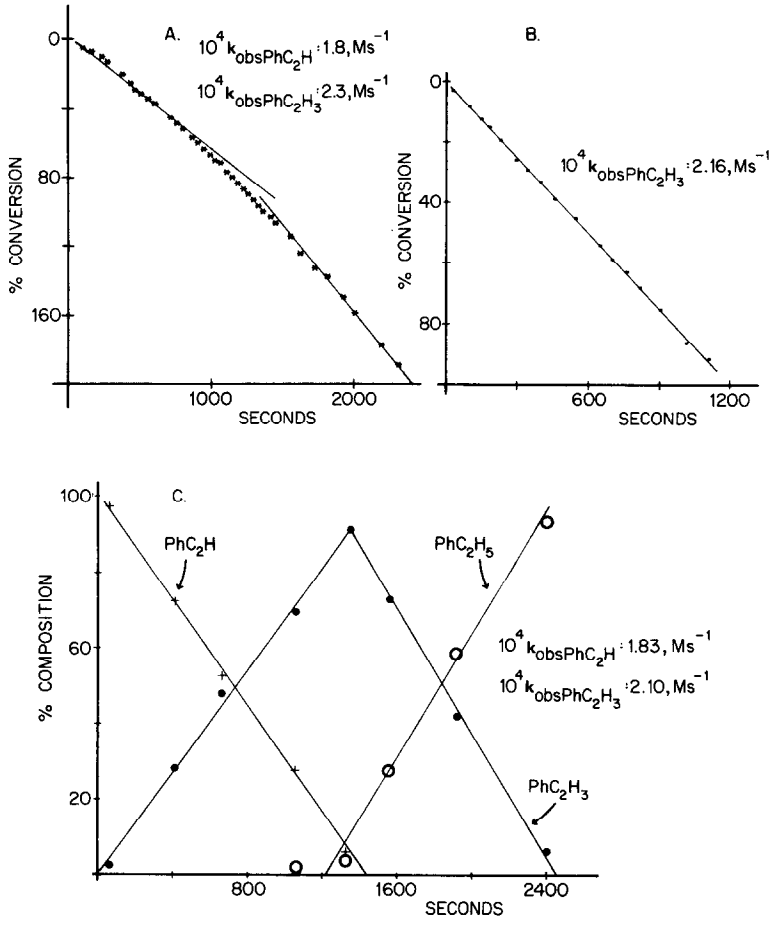

FIG. 7. Hydrogenation experiments with catalyst B_2, 1 atm P_{H_2}, t = 25°C, substrate = 0.26 M; solvent, n-heptane 10 ml; catalyst, 67 mg; (A) volumetric hydrogenation of PhC_2H; (B) volumetric hydrogenation of PhC_2H_3; (C) hydrogenation of PhC_2H from GLC.

TABLE 2

Hydrogenation of PhC_2H[a]

Catalyst	P_{H_2} (atm)	$10^4 \cdot k_{obs\ PhC_2H}$ (M sec^{-1} mg_{Pd}^{-1})	$10^4 \cdot k_{obs\ PhC_2H_3}$ (M sec^{-1} mg_{Pd}^{-1})	Selectivity[b] (±2%)
A_1	1	3.99	5.14	100
A_2	1	4.02	5.01	100
A_3	1	3.84	4.95	100
B_1	1	2.05	2.19	94
B_2	1	1.91	2.00	91
B_2	5	6.2	—	80
B_2	10	15.2	—	76
B_2	20	20.9	—	72
C_1	1	1.55	—	78
C_2	1	1.25	—	71

[a] Rate constants per mg of Pd, t = 25°C, [PhC_2H] = 0.26 M, solvent n-heptane 10 ml.

[b] Selectivity = 100× % PhC_2H_3/% PhC_2H_3 + % PhC_2H_5. % PhC_2H_3 kept at the maximum value during each kinetic run.

are larger than the corresponding $k_{obs\ PhC_2H}$. Nevertheless the kinetic behaviours were quite different among the used catalysts.

For the catalysts of type A the hydrogenation of styrene started after 100% of phenylacetylene was half-hydrogenated; whereas in the case of the catalysts B_1 and B_2 at some interval of the kinetic run PhC_2H, PhC_2H_3, and PhC_2H_5 were simultaneously present (Fig. 7C). This tendency becomes more marked for catalysts C_1 and C_2 where ethylbenzene is present even at the beginning of the reaction (Fig. 8). This is obviously related to the selectivity which becomes smaller on going from catalysts of type A to B and C.

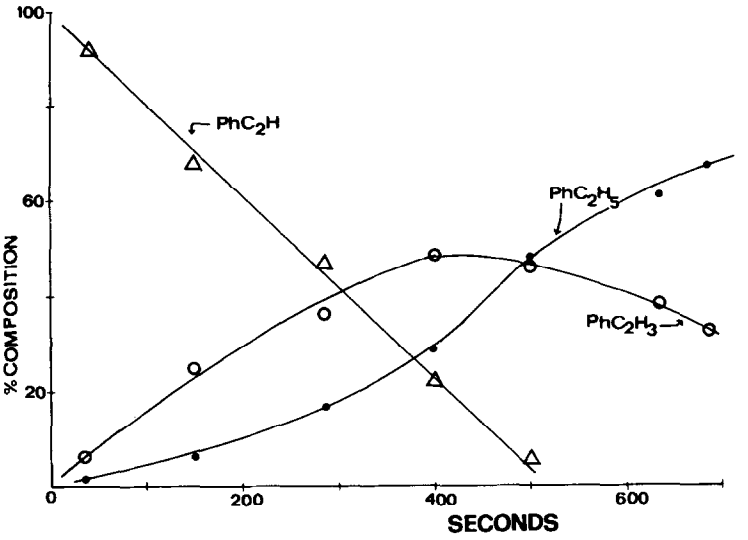

FIG. 8. Hydrogenation of PhC_2H with catalyst B_2 (70 mg): PhC_2H = 0.26 M, solvent, n-heptane 10 ml, 5 atm P_{H_2}.

Catalysts A_1, A_2, and A_3 are the best catalysts in terms of catalytic activity and selectivity; highest metal dispersions display the higher ratio of $k_{obs\ PhC_2H_3}/k_{obs\ PhC_2H}$. Since for both PhC_2H and PhC_2H_3 hydrogenations the pseudo-zeroth order behavior was rigorously respected, the H_2 activation should be, as generally accepted in these cases (*23*, *37*), the rate-determining step for both reactions. Thus, selectivity should arise from the favorable competition of PhC_2H with respect to PhC_2H_3 on coordinating the active centers. A mechanism accounting for these results is presented in Scheme 1 in the hypothesis that $k_1 \gg k_2$.

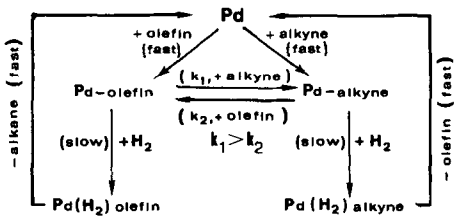

This reaction mechanism is substantially the "unsaturate route" for olefin hydrogenation in homogeneous systems (*38*) and it may be extended to heterogeneous catalysis if the Pd particle dimensions are small enough so that the metal could be considered dispersed at the level of metallic clusters of a relatively small number of atoms. In the case of Pd catalysts, the presence of very high dispersions excludes considerable amounts of hydrogen dissolved in the particles during the catalytic experiments (*12*). According to the thermodynamics of the Pd–H system, the transition of α-Pd hydride $\rightarrow$ β-Pd hydride may occur both for small and large particles; but experimental evidence has shown that in very small particles the occurrence of the β-Pd hydride phase is less easy (*9*, *13–15*). Indeed X-ray diffraction analysis carried out on samples of type A after the catalytic run does not show any appreciable shift of the peaks of the α-Pd to the β Pd-H phase, although the high Pd dispersion prevents the determination of the lattice parameter (Fig. 2).

In the above scheme, the selectivity arises from the statement that $k_1 \gg k_2$; hence it is directly related to the different strengths of the Pd metal–alkyne with respect to Pd metal–olefin bonds.

In the majority opinion the metal surface–acetylenes bond is considered much stronger than the corresponding bond with olefins, but the electronic interactions have

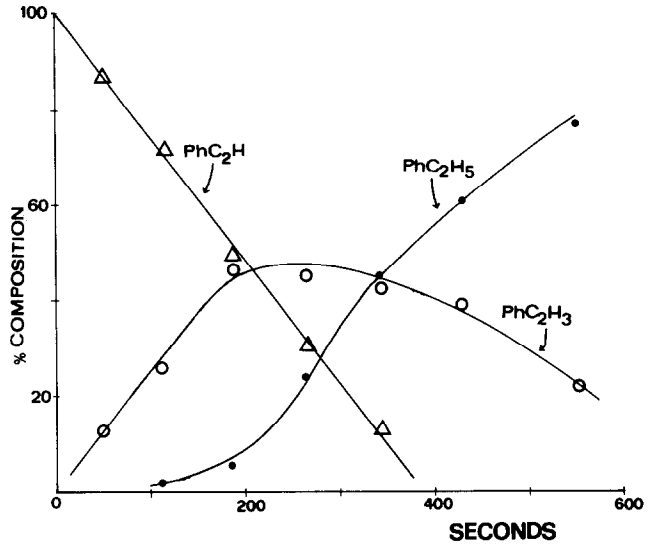

FIG. 9. Hydrogenation of PhC_2H with catalyst C_2 (80 mg): PhC_2H = 0.26 M, solvent, n-heptane 10 ml, 1 atm P_{H_2}, t = 25°C.

often been similarly described without any relevant feature taking account of their different strength. Moreover, a direct comparison is sometimes made with the organometallic counterparts, and in particular with the d^8 metal complexes.

The bonding of d^{10} metal ions with olefins and acetylenes is surely more likely compared with the bonding interactions between these unsaturated molecules and the small particle palladium metal surface. As a matter of fact, the correlations between organometallic compounds and metal surface chemistry may be useful for a better understanding of heterogeneous catalysis processes (*39, 40*), but these must be restricted within the appropriate bonds (*41*).

Olefins and acetylenes are bound quite differently to d^{10} transition metal ions. In the former case the bond may be weaker than the normal π bonding to d^8 metal ions since the contribution to the bond of the back donation from the metal filled d orbitals to the empty antibonding orbitals of the olefinic bond should be reduced. In fact, d^{10} metal ions use coordination geometries unfavorable to the best overlap among the available π orbitals. Alternatively, the d^{10} metal ion–acetylene bonding mode has been described in a different way; this justifies the larger strength of the bond, since acetylenes are bonded to the metal through two σ metal carbon bonds (*42–45*). These two bonding situations may find a valid counterpart in the Pd metal surface chemistry and explain the larger thermodynamic adsorptive factor of acetylenes with respect to monoolefins. Although the nature of the acetylene–metal surface interactions is still an open argument, on the basis of spectroscopic data (*46–50*) the acetylene–metal surface bond is known to involve an extensive rehybridization of the C≡C moiety with a large reduction of the bond order, in agreement with possible formation of two σ metal–carbon bonds. Moreover, it has been demonstrated that ethylene is essentially present as π-adsorbed on Pd, Pt, and Rh surfaces (*51*). This metal–olefin bond is weaker than the bond constituted by two σ metal–carbon bonds and it is easily destroyed by H_2. Consistent with this latter point, the values of $k_{\text{obs } PhC_2H_3}$ are larger than the values of $k_{\text{obs } PhC_2H}$ (Table 2).

The metal particle size distributions obtained for catalysts of type B and C (Figs. 4

and 5) indicate a different morphological situation. Thus, a considerable fraction of the Pd loaded on catalysts B_1, B_2, C_1, and C_2 is constituted by particles larger than those of the type A. Parallel to this, the catalytic activity is lower for both PhC_2H and PhC_2H_3 hydrogenation; the alkyne half-hydrogenation is still a pseudo-zero order reaction, but the kinetic behavior in the case of catalysts C_1 and C_2 prevents the determination of $k_{\text{obs } PhC_2H_3}$.

The selectivity of catalysts B and C is generally lower than the one of catalysts A and it becomes smaller as the average metal particle size is increased. The considerations reported for catalysts A may be extended to the fraction of Pd metal particles of catalysts C and B smaller than 30 Å in diameter, but the presence of dissolved hydrogen cannot be neglected for the largest particles during the kinetic run. The catalytic experiments at high pressures of hydrogen show that (i) the rate of half-hydrogenation increases with the pressure, (ii) the selectivity is lowered with respect to the experiments at 1 atm, and (iii) styrene hydrogenation does not follow a zero-order kinetic (Fig. 9). These results suggest that in the case of catalysts holding metal particles larger than 30 Å the hydrogenation reaction should involve elementary steps different from Scheme 1.

The presence of a large H content inside the metal during the catalytic process may change the attack of the unsaturated substrate to the metal surface in the sense that it may be more reasonably compared to the insertion on the Pd–H bond than to a coordination on a d^{10} metal ion. Indeed, the difference of strength of the Pd metal–alkyne and Pd metal–olefin bonds should be larger than the different insertion ability of olefins and alkynes into the Pd-H bond, therefore accounting for the lower selectivity observed for catalysts B and C. It is noteworthy that the selectivity in the alkyne half-hydrogenation with polymer bound Pd(II) compounds (*52*) does not reach 100% of selectivity, and also in this case the Pd–H unit was considered as the reactive species. In agreement with these considerations the ratio $k_{\text{obs } PhC_2H_3}/k_{\text{obs } PhC_2H}$ is smaller for catalysts B_1 and B_2 than for catalysts A.

In agreement with the Wells approach (*12*), a further important factor contributing a lower selectivity as the Pd particle size increases is the β Pd-hydride phase which may furnish the required amount of hydrogen to the styrene molecule before it leaves the active center, to give the saturated alkane. The results obtained at high H_2 pressure agree with this.

It is interesting to note that the results presented here and discussed are in good agreement with findings of Palczewska *et al.* (*9*) obtained under quite different experimental conditions and using conventional catalysts. This gives further support to our conclusion that the selective half-hydrogenation of alkynes with Pd catalysts is favored by very high metal dispersions and low hydrogen pressures. The achievement of a good selectivity arises from the strong bonding interactions of the C≡C group to the α Pd phase; the presence of β Pd hydride reduces the difference between alkynes and olefins as coordinating agent with consequent reduction of the selectivity.

ACKNOWLEDGMENTS

CNR, Rome, is acknowledged for financial support (Progetti Finalizzati-Chimica Fine e Secondaria).

REFERENCES

1. U.S. Pat., 2,250,925(29.7.41.); *Chem. Abstract.* **35,** 6983 (1941).
2. Spector, M. L., and Heinemann, H., *Chem. Ing. Techn.* **34,** 120 (1962).
3. Asinger, F., "Mono-olefin Chemistry and Technology." Pergamon Press, Oxford, 1968.
4. Bond, G. C., and Wells, P. B., *Adv. Catal.* **15,** 91 (1964).
5. Allison, E. G., and Bond, G. C., *Catal. Rev.* **7,** 233 (1973).
6. Lindlar, H., and Dubuis, R., *Org. Syn.* **46,** 89 (1966).
7. Siegel, S., *Adv. Catal.*, **16,** 160 (1966).
8. Bond, G. C., Dowden, D. A., and McKenzie, N., *Trans. Faraday Soc.* **54,** 1537 (1958).
9. Palczewska, W., *Adv. Catal.* **24,** 245 (1975).

10. Borodzinski, A., Dus, R., Frank, R., Janko, A., and Palczewska, W., *Proc. Int. Conf. Catal. 5th*, A7, London (1976).
11. Janko, A., Palczewska, W., and Szmerska, I., *J. Catal.* **61,** 264 (1980).
12. Wells, P. B., *J. Catal.* **52,** 498 (1978).
13. Aben, P. C., *J. Catal.* **10,** 224 (1968).
14. Boudart, M., and Hwang, H. S., *J. Catal.* **39,** 44 (1975).
15. Benedetti, A., Cocco, G., Enzo, S., Pinna, F., and Schiffini, L., *J. Chim. Phys.* **78,** 875 (1981).
16. Carturan, G., Cocco, G., Schiffini, L., and Strukul, G., *J. Catal.* **65,** 359 (1980).
17. Pope, D., Smith, W. L., Eastlake, M. G., and Moss, A. R., *J. Catal.* **22,** 72 (1971).
18. Cocco, G., Schiffini, L., Strukul, G., and Carturan, G., *J. Catal.* **65,** 348 (1980).
19. Benedetti, A., Cocco, G., Enzo, S., Piccaluga, G., and Schiffini, L., *J. Chim. Phys.* **78,** 961 (1981).
20. Cocco, G., Enzo, S., Schiffini, L., and Carturan, G., *J. Mol. Catal.* **11,** 161 (1981).
21. O'Brien, S., Fishwick, M., McDermott, B., Wallbridge, M. G. H., and Wright, G. A., *Inorg. Synth.* **XIII,** 73 (1972).
22. Carturan, G., Gottardi, V., and Graziani, M., *J. Non-Crystall. Solids* **29,** 41 (1978).
23. Carturan, G., and Gottardi, V., *J. Mol. Catal.* **4,** 349 (1979).
24. Carturan, G., and Strukul, G., *J. Catal.* **57,** 516 (1979).
25. Kratky, O., Pilz, I., and Schmitz, P. J., *J. Colloid. Interface Sci.* **21,** 24 (1966).
26. Porod, G., *Kolloid. Z.* **124,** 83 (1951); **125,** 51 (1952).
27. Guinier, A., and Fournet, G., "Small Angle X-ray Scattering." Wiley, New York, 1955.
28. Vonk, C. G., *J. Appl. Crystallogr.* **9,** 433 (1976).
29. Sashital, S. R., Cohen, J. B., Burwell, R. L., and Butt, J. B., *J. Catal.* **50,** 479 (1977).
30. Guinier, A., "X-ray Diffraction." W. H. Freeman and Company, San Francisco, 1963.
31. Warren, B. E., and Averbach, B. L., *J. Appl. Phys.* **21,** 595 (1950).
32. Ganesan, P., Kuo, H. K., Saavedra, A., and De Angelis, R. J., *J. Catal.* **52,** 310 (1978).
33. Bertaut, E. F., *Acta Crystallogr.* **3,** 14 (1950).
34. Lewis, F. A., "The Palladium Hydrogen System." Academic Press, London, 1975.
35. Kieboon, A. P. G., and Van Bekkum, H., *J. Catal.* **25,** 342 (1973).
36. Caga, I. T., Shutt, E., and Winterbotton, J. M., *J. Catal.* **44,** 271 (1976).
37. Fuji, Y., and Bailar, J. C., Jr., *J. Catal.* **52,** 342 (1978).
38. James, B. R., "Homogeneous Hydrogenation," Chap II. Wiley-Interscience, New York, 1973.
39. Siegel, S., *J. Catal.* **30,** 139 (1973).
40. Ugo, R., *Catal. Rev.* **11,** 225 (1975).
41. Moskovits, M., *Acc. Chem. Res.* **12,** 229 (1979).
42. Collman, J. P., and Kang, J. W., *J. Amer. Chem. Soc.* **89,** 844 (1967).
43. Granville, J. O., Stewart, J. M., and Grim, S. O., *J. Organometal. Chem.* P9 (1967).
44. Ittel, S. D., and Ibers, J. A., *Adv. Organomet. Chem.* **14,** 33 (1976).
45. Otsuka, S., and Nakamura, A., *Adv. Organomet. Chem.* **14,** 245 (1976).
46. Demuth, J. E., *Chem. Phys. Lett.* **45,** 12 (1977).
47. Demuth, J. E., *Surf. Sci.* **80,** 367 (1979).
48. Ozin, G. A., McIntosh, D. F., Power, W. J., and Messmer, R. P., *Inorg. Chem.* **20,** 1782 (1981).
49. Ibach, H., Hopster, H. and Sexton, N., *App. Surf. Sci.* **1,** 1 (1977).
50. Lehwald, S., Erly, W., Ibach, H., and Wagner, H., *Chem. Phys. Lett.* **62,** 360 (1979).
51. Soma, Y., *J. Catal.* **59,** 239 (1979).
52. Teresawa, M., Yamamoto, H., Kaneda, K., Imanka, T., and Teranishi, S., *J. Catal.* **57,** 315 (1979).